

## PHASE TRANSITION IN HYDRAZINIUM HYDROGEN OXALATE. A CALORIMETRIC STUDY OF THE SHORT HYDROGEN BOND SYSTEM \*

TAKASUKE MATSUO and HIROSHI SUGA

*Department of Chemistry and Chemical Thermodynamics Laboratory, Faculty of Science,  
Osaka University, Toyonaka, Osaka 560 (Japan)*

(Received 29 July 1986)

### ABSTRACT

The heat capacity of hydrazinium hydrogen oxalate crystal has been measured between 14 and 300 K. A first-order phase transition was found at 217.6 K. Total transition enthalpy and entropy are  $1.09 \text{ kJ mol}^{-1}$  and  $4.18 \text{ J K}^{-1} \text{ mol}^{-1}$ , respectively. The high temperature phase supercooled to 165–170 K. The heat capacity of the supercooled high temperature phase was significantly larger than that of the low temperature phase. By fitting a Schottky heat capacity function to the heat capacity difference, a Schottky energy level was found at  $(135 \pm 4) \text{ cm}^{-1}$  above the ground state and related to the tunneling splitting of the energy levels of the short acidic hydrogen bond. A thermodynamic model of the first-order transition is proposed in which the Schottky anomaly plays the main role. Far-infrared spectra of hydrazinium hydrogen oxalate are reported for the frequency range  $400\text{--}30 \text{ cm}^{-1}$  at temperatures of 295 and 90 K.

### INTRODUCTION

Hydrogen bonds in acidic salts are often very short and give rise to various interesting structural and spectroscopic features in the crystals containing them. The most thoroughly studied compounds of this type are  $\text{KH}_2\text{PO}_4$  and its homologs. Important theoretical concepts, such as double minimum potentials, tunneling motion and vertex models, found practical applications in them. A number of acidic salts of carboxylic acids are known to form crystals containing short hydrogen bonds. In these compounds, the carbon chain of the acid molecules adds a variable element and complication in the structure that do not exist in the ferroelectric phosphates. The symmetry of the crystals of the organic acidic salts is usually low (mono-

---

\* Dedicated to Professor Syûzô Seki in honor of his contribution to calorimetry and thermal analysis.

Contribution No. 110 from the Chemical Thermodynamics Laboratory.

clinic or triclinic) as compared with the tetragonal symmetry of  $\text{KH}_2\text{PO}_4$ .

Dicarboxylates, of which the present compound hydrazinium hydrogen oxalate (HYHOX) is a member, are interesting structurally and thermophysically because the two acid groups give them the capability of forming hydrogen-bonded chains.

The crystal structure of HYHOX was determined by X-ray and neutron diffraction to an unusual detail [1-4]. Both the hydrazinium  $\text{NH}_3^+ - \text{NH}_2$  and oxalate  $(\text{CO}_2)_2^{2-}$  can form hydrogen bonds. In fact, all the atoms, except for carbon, take part in the hydrogen bond, forming  $\text{O}-\text{H}-\text{O}$ ,  $\text{O} \cdots \text{H}-\text{N}$  and  $\text{N}-\text{H} \cdots \text{N}$  bonds. The  $\text{O}-\text{H}-\text{O}$  bond is symmetric with the center of symmetry at the center of the bond. The  $\text{O}-\text{O}$  distance is 0.2457 nm as determined by the neutron. For comparison the  $\text{O}-\text{O}$  distance in ice Ih is 0.276 nm and that in  $\text{KH}_2\text{PO}_4$  is 0.25 nm.

The electron distribution in the  $\text{O}-\text{H}-\text{O}$  bond of HYHOX, determined by X-ray diffraction, has two maxima 0.104 nm apart from each other [3]. The proton distribution, on the other hand, has a broad maximum [4], which is consistent with symmetric double maxima separated by 0.025 nm [4]. Thus, the hydrogen bond in HYHOX belongs to a borderline case between the single minimum and double minima types.

The existence of labile hydrogens is characterized by an extremely broad absorption in the infrared spectrum in the solid state [5] and by a continuous absorption in the liquid state [6]. Such absorption has been found in the IR spectrum of HYHOX [7].

If the proton distribution is statistical, as the double-peaked electron density suggests [3], one should expect that the crystal undergoes a phase transition to an ordered state at a lower temperature. In fact a phase transition accompanied by doubling of the unit cell occurs at approximately  $-100^\circ\text{C}$  [1].

The motion of the hydrazinium ion was studied by nuclear magnetic resonance (NMR) (absorption second moment [8] and spin-lattice relaxation [9]). The two methods agree that the hydrazinium reorients rapidly at room temperature and becomes rigid at lower temperatures. No anomaly was found at the suspected transition temperature.

In this paper we present the low temperature heat capacity of the compound that shows the occurrence of the phase transition at 217.6 K, and analyze the data to derive a model of the phase transition in which the short hydrogen bond plays the major role.

## EXPERIMENTAL

The compound was prepared after ref. 10 and recrystallized from hot aqueous solution. The chemical analysis gave: C, 19.6% (calc. 19.68); H, 4.93% (4.95); N, 23.3% (22.95); oxalate, 72.4% (72.10). The calorimeter used

for the measurement was described in ref. 11. The sample mass was 18.420 g. In the course of measurement, it was found that the high temperature phase supercooled to various degrees depending on the thermal history of the sample. In order to fully convert the sample into the low temperature phase it was kept at a low temperature for 20 days.

Differential thermal analysis was employed to determine the temperature of the stability limit of the high temperature phase. It was found that the high temperature phase (stable above 217 K) could be supercooled to 165–170 K. The heat capacity of the supercooled high temperature phase was also measured. The far-infrared spectrum was recorded ( $400\text{--}30\text{ cm}^{-1}$ ) at room temperature and 90 K.

## RESULTS AND DISCUSSION

The heat capacity data are given in Table 1 and plotted in Fig. 1. They are given in the unit of the gas constant,  $R = 8.3144\text{ J K}^{-1}\text{ mol}^{-1}$ . The peak due to the phase transition occurred at 216.3, 217.4 and 219.2 K in the different series of measurement. The average temperature was 217.6 K. The transition is rather broad ( $\Delta T \approx 10\text{ K}$ ), even though it is a first-order transition as the supercooling shows. The heat capacity data around the transition temperature are shown at an enlarged scale in Fig. 2. The data were obtained on the most thoroughly stabilized low temperature phase and the supercooled high temperature phase. They are remarkably different from each other where they overlap. Such a difference is usually associated with a drastic change of mobility of molecules as in the rigid-to-plastic phase changes and was unexpected in HYHOX which is an extensively hydrogen-bonded crystal.

### *Vibrational heat capacity*

It is necessary to calculate the vibrational heat capacity in order to derive the enthalpy and the entropy of the transition and any excess heat capacity related to hydrogen-bond disorder. The vibrational heat capacity can be calculated by use of the Einstein heat capacity functions if all the vibrational frequencies are known. Since this is not the case for the present substance, we employed a combination of the Debye and Einstein functions to express the total vibrational heat capacity. The characteristic frequencies were determined from the vibrational spectra and by a least-squares fitting of the heat capacity function to the experimental values.

The unit cell of HYHOX contains two formula units [1–3]. Therefore the vibrational model should in principle be enumerated accordingly. However, we analyzed the heat capacity for one mole of HYHOX (rather than one mole of the unit cell) on the assumption that the correlation splitting is smaller than the thermal energy for  $T > 14\text{ K}$ .

TABLE 1

Molar heat capacity of hydrazinium hydrogen oxalate

$T$ (K)	$C_p$ (R)	$T$ (K)	$C_p$ (R)	$T$ (K)	$C_p$ (R)	$T$ (K)	$C_p$ (R)
144.55	11.620	279.81	18.13	189.04	13.979	32.37	1.891
148.74	11.863	284.79	18.34	192.90	14.139	33.32	2.019
152.87	12.091	289.73	18.55	189.05	13.905	34.44	2.138
156.33	12.274	294.62	18.76	192.77	14.106	35.53	2.273
159.37	12.435	299.47	18.96	196.46	14.292	36.80	2.520
162.55	12.607			200.10	14.746	38.43	2.628
165.68	12.775	196.00	14.489	203.70	14.726	40.15	2.842
168.77	12.941	199.17	14.590	206.38	15.03	41.89	3.051
171.85	13.106	201.80	14.720	208.14	15.35	43.97	3.305
174.88	13.273	204.85	14.855	209.87	15.98	46.22	3.576
177.89	13.432	208.30	15.01	211.53	17.70	48.78	3.876
180.86	13.594	211.74	15.17	213.12	18.69	51.54	4.214
183.82	13.756	215.13	15.32	214.61	22.25	54.11	4.510
186.74	13.898	218.51	15.48	215.95	26.57	56.49	4.777
178.56	13.430	221.86	15.62	217.14	32.22	83.38	7.355
181.69	13.585	225.19	15.78	218.26	31.11	87.54	7.693
184.69	13.733			219.56	20.33		
187.20	13.878	80.89	7.160	221.41	16.66	129.80	10.642
190.22	14.033	84.59	7.474	223.66	15.77	132.74	10.825
193.32	14.208	88.14	7.770	225.64	15.75	135.65	10.998
196.49	14.394	91.56	8.043			181.90	13.548
199.62	14.497	94.87	8.299	56.96	4.828	184.93	13.709
202.72	14.820	98.10	8.537	60.60	5.216	188.68	13.906
205.78	15.37	101.19	8.770	64.45	5.608	193.04	14.168
208.78	15.81	104.24	8.989	68.01	5.960	196.28	14.282
211.65	18.56	107.21	9.203	71.34	6.267	130.67	10.691
214.14	24.41	110.12	9.403	74.51	6.569	133.59	10.869
216.33	28.60	113.11	9.607	77.86	6.874	136.47	11.046
218.75	17.99	116.93	9.861	81.41	7.178		
221.60	15.66	121.41	10.151			79.97	7.048
224.55	15.76	125.82	10.433	14.24	0.219	84.31	7.417
227.41	15.89	130.14	10.702	15.67	0.293	88.42	7.754
230.32	16.02	133.77	10.921	16.56	0.345	92.37	8.063
233.21	16.15	136.80	11.086	17.51	0.405	96.18	8.353
236.04	16.26	139.78	11.278	18.48	0.475	98.98	8.569
238.95	16.39	142.36	11.434	19.35	0.538	102.57	8.826
241.96	16.52	145.61	11.608	20.22	0.609	106.89	9.136
245.16	16.65	149.90	11.863	21.11	0.683	111.92	9.479
248.29	16.78	154.12	12.097	22.09	0.770	116.80	9.806
251.43	16.92	158.27	12.323	23.16	0.870		
254.54	17.05	162.36	12.545	24.18	0.972	121.52	10.114
257.64	17.19	166.07	12.739	25.15	1.069	126.12	10.406
260.68	17.30	169.72	12.937	26.25	1.186	130.61	10.683
263.77	17.44	173.66	13.149	27.48	1.322	135.00	10.950
266.81	17.59	177.54	13.360	28.74	1.463	139.30	11.208
272.83	17.82	181.39	13.572	30.05	1.615	139.67	11.234
275.82	17.98	185.19	13.768	31.26	1.758	143.87	11.479

TABLE 1 (continued)

$T$ (K)	$C_p$ (R)	$T$ (K)	$C_p$ (R)	$T$ (K)	$C_p$ (R)	$T$ (K)	$C_p$ (R)
148.01	11.717	200.76	14.529	236.27	16.26	184.31	13.880
152.29	11.958	204.95	14.879	240.11	16.44	188.48	14.085
156.70	12.199	209.07	15.58	243.59	16.73	192.60	14.276
161.05	12.437	212.94	18.31	247.72	16.76	196.90	14.491
165.33	12.665	216.33	24.84			201.14	14.683
169.78	12.908	219.22	29.66	162.68	12.756	206.44	14.931
174.39	13.149	222.54	16.48	167.13	13.006	212.95	15.25
178.81	13.382	225.47	15.80	171.50	13.242	219.37	15.51
183.28	13.611	228.44	15.90	175.83	13.467	224.91	15.75
192.19	14.079	232.38	16.09	180.10	13.675	229.60	15.96
196.50	14.307						

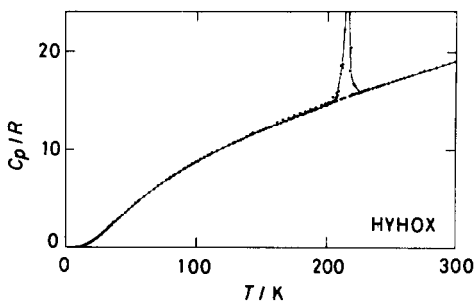


Fig. 1. Heat capacity of hydrazinium hydrogen oxalate crystal.

The 42 ( $= 14 \times 3$ ) degrees of freedom of HYHOX are divided into the internal vibrations of  $\text{NH}_3^+ - \text{NH}_2$  and  $\text{HC}_2\text{O}_4^-$  and their external vibrations. The internal vibrations have been studied by infrared spectroscopy and

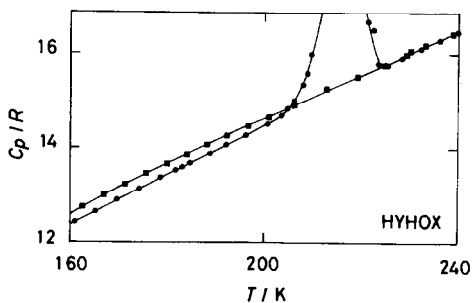


Fig. 2. Heat capacity of hydrazinium hydrogen oxalate in the stable and meta-stable phases.

TABLE 2

Vibrational frequencies used in the heat capacity calculation (from refs. 12–16)

Frequency ( $\text{cm}^{-1}$ )	Weight		Frequency ( $\text{cm}^{-1}$ )	Weight	
<i>Hydrazinium ion</i>		$\text{NH}_3^+ - \text{NH}_2$	<i>Oxalate</i>		$(\text{COO})_2^{2-}$
3150	2	$\nu(\text{NH}) - \text{NH}_2$	1402	1	$\nu_s(\text{COO}^-)$
2950	1	$\nu(\text{NH}) \left. \vphantom{\nu(\text{NH})} \right\} - \text{NH}_3$	1259	1	$\nu(\text{C}-\text{O})$
2716	2	$\nu(\text{NH}) \left. \vphantom{\nu(\text{NH})} \right\} - \text{NH}_3$	882	1	$\nu(\text{C}-\text{C})$
1614	1	$\delta(\text{HNNH}) \text{NH}_2$	724	1	$\delta(\text{COO})$
1500	1	$\delta(\text{HNNH}) \text{NH}_3$	578	1	$\rho(\text{COO})$
1417	2	$\delta(\text{HNNH}) \text{NH}_3$	505	1	$\delta(\text{COO})$
1124	2	$\rho \left. \vphantom{\rho} \right\} \text{NH}_3, \text{NH}_2$	492	1	$\rho(\text{COO})$
1101	2	$\rho \left. \vphantom{\rho} \right\} \text{NH}_3, \text{NH}_2$	335	1	wag(COO)
973	1	$\nu(\text{N}-\text{N})$	239	1	wag(COO)
504	1	int. rotation	–	1	twist
<i>Oxalate</i>			<i>O-H-O</i>		
1725	1	$\nu(\text{C}=\text{O})$	1435	1	$\delta(\text{OH})$
1640	1	$\nu_s(\text{COO}^-)$	1041	1	$\gamma(\text{OH})$
			1880	1	$\nu(\text{OH})$

normal mode calculation [7,12–15]. The frequencies used in the heat capacity calculation are given in Table 2. The frequencies associated with the acidic protons were taken from a related compound,  $\text{NaH}(\text{CO}_2)_2\text{H}_2\text{O}$  [16]. The frequency of the internal rotation of the hydrazinium ion has been derived neither experimentally nor from calculation. But the activation energy of  $-\text{NH}_3^+$  has been given:  $8.1 \text{ kcal mol}^{-1}$  [8] and  $8.4 \text{ kcal mol}^{-1}$  [9]. By representing the activation energy with a three-fold sinusoidal potential, we obtained the vibrational frequency  $504 \text{ cm}^{-1}$  in the harmonic approximation. The moment of inertia was calculated from the crystal structure [2,3]. Only  $-\text{NH}_3^+$  was assumed to rotate because the  $-\text{NH}_2$  end of the hydrazinium ion is rigidly hydrogen-bonded [17]. The zero-point vibration was taken into account in the calculation. The vibrational period corresponding to  $504 \text{ cm}^{-1}$  is equal to  $10.5 \text{ fs}$  and close to the experimental pre-exponential factor  $\tau_0 = 8.0 \text{ fs}$  [9].

There are twelve external vibrations. Their frequencies are not known. One of the oxalate's internal vibrations (twisting) has also not been assigned. They were determined by a least-squares fitting as follows. The function minimized was

$$F(\nu_D, \nu_{E1} \dots \nu_{E4}, A) = \sum_i \left[ C_p(T_i) - A(C_p(T_i))^2 - C_v(\text{calc}) - C_v(\text{fit}) \right]^2$$

Here  $C_v(\text{calc})$  = the harmonic oscillator heat capacities summed over the

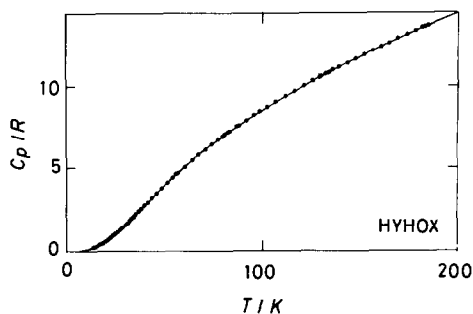


Fig. 3. Heat capacity of the low temperature phase of hydrazinium hydrogen oxalate and the best-fit vibrational heat capacity (—).

modes given in Table 2;  $C_v(\text{fit}) = 3RD(\nu_D/T_i) + 3R\sum_{j=1}^3 E(\nu_{Ej}/T_i) + RE(\nu_{E4}/T)$ , where  $R$  is the gas constant,  $D(\nu_D/T_i)$  the Debye function of the Debye frequency  $\nu_D$  at  $T = T_i$  and  $E(\nu_{Ej}/T_i)$  the Einstein function of the Einstein frequency  $\nu_{Ej}$  at  $T = T_i$ ;  $A(C_p(T_i))^2 =$  the  $C_p - C_v$  correction term.

The six parameters ( $\nu_D$ ,  $\nu_{E1} \dots \nu_{E4}$  and  $A$ ) were determined by minimizing  $F$  for the 74 heat capacity data between 14 and 185 K of the low temperature phase. The fitted curve is shown in Fig. 3 and the optimized parameter values are given in Table 3. The standard deviation of the fit was  $0.051 \text{ J K}^{-1} \text{ mol}^{-1}$ .

### Enthalpy and entropy of transition

The bulk of the enthalpy and entropy changes occurred in the  $\sim 10 \text{ K}$  interval around 217.6 K. The magnitude of the changes depended on the sample history. Since the heat capacity of the high temperature phase was reproducible, the different values of the transition enthalpy are due to incomplete conversion of the high temperature to the low temperature phase. The entropy changes obtained in the four series of measurement are plotted in Fig. 4. The zero value of the entropy was taken to be at infinite temperature. The largest change,  $0.503R = 4.18 \text{ J K}^{-1} \text{ mol}^{-1}$ , was obtained

TABLE 3

Optimized Debye, Einstein and  $C_p - C_v$  parameters of the heat capacity function

Frequency ( $\text{cm}^{-1}$ )	$\nu_D$	$\nu_{E1}$	$\nu_{E2}$	$\nu_{E3}$	$\nu_{E4}$
	$103 \pm 2$	$143 \pm 2$	$176 \pm 2$	$392 \pm 2$	$86 \pm 3$
Weight	3	3	3	3	1
$A$ ( $\text{mol J}^{-1}$ )	$(8.5 \pm 2) \times 10^{-7}$				

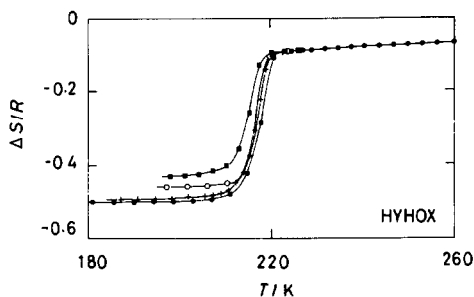


Fig. 4. Entropy of transition of hydrazinium hydrogen oxalate crystal obtained on the sample annealed for different times at low temperature.

on the sample annealed for 20 days. The corresponding enthalpy change was  $1.09 \text{ kJ mol}^{-1}$ .

#### *Model of the phase transition in HYHOX*

The acidic hydrogen in HYHOX has a double maxima distribution in the X-ray diffraction model whereas it has a single, centered position in the neutron diffraction model [3,4]. The occurrence of the phase transition and its entropy change,  $0.503R$ , suggest that the room temperature structure is of statistical nature. It was pointed out that the broad, single peak in the neutron result may have two hidden maxima [4].

The phase transition can be related to the disorder in a thermodynamic argument as follows. In the high temperature phase the hydrogen atoms occupy one of the two equivalent positions on the hydrogen bond, without correlation with each other. At a low temperature, the decrease of the free energy due to the entropy associated with the random distribution of the protons becomes less than the average energy associated with the random distribution. Below that temperature the ordered state becomes more stable than the disordered state and the phase change occurs. The ordered phase seems to be realized in the deuterated analog of HYHOX [3]. However, whether or not the same ordered structure occurs in HYHOX is not known. It is more probable that they are different [1,3].

When the maxima of the distribution of the hydrogen atom in the hydrogen bond are near to each other, one should expect a tunneling splitting of the two ground states (corresponding to occupation of either of the two positions) into symmetric and antisymmetric states, even though there seems to be no exact formulation that relates the O–O distance with the magnitude of the splitting. Since tunneling splitting does not occur in the ordered phase, it is reasonable to associate the heat capacity difference (Fig. 2) with tunneling splitting.

The excess heat capacity determined by subtraction of the best-fit low temperature heat capacity function from the heat capacity of the high



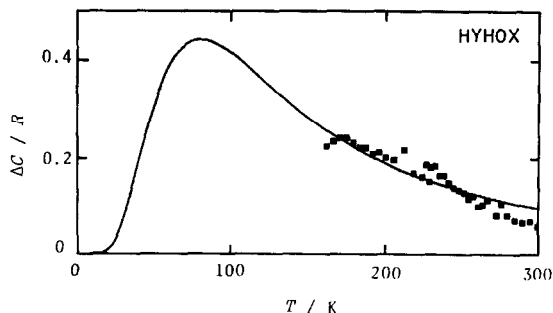


Fig. 5. Excess heat capacity of hydrazinium hydrogen oxalate and the best-fit Schottky heat capacity (—).

temperature phase in its stable and metastable temperature regions was compared with a two-level Schottky function,

$$\frac{\Delta C}{R} = \left( \frac{T_0}{T} \right)^2 \frac{\exp(-T_0/T)}{[1 + \exp(-T_0/T)]^2}$$

The parameter  $T_0$  was determined by the least-squares method:  $T_0 = (195 \pm 5)$  K ( $= 135 \pm 4$  cm<sup>-1</sup>). The fitting is shown in Fig. 5. Extrapolation to infinite temperature, necessary for the entropy calculation (Fig. 4), was made by use of the Schottky function. We can now use the Schottky function in the thermodynamic description of the phase transition. Since the entropy of the ordered phase is zero, its Helmholtz energy  $A_L$  is equal to the internal energy  $U_0$ . The Helmholtz energy  $A_H$  of the tunneling phase is given by

$$A_H = -RT \ln[1 + \exp(-T_0/T)]$$

Equating  $A_L$  and  $A_H$  at  $T = 217.6$  K, we obtain  $U_0 = -616$  J mol<sup>-1</sup>. This is the energy of the localized ordered state relative to the tunneling ground

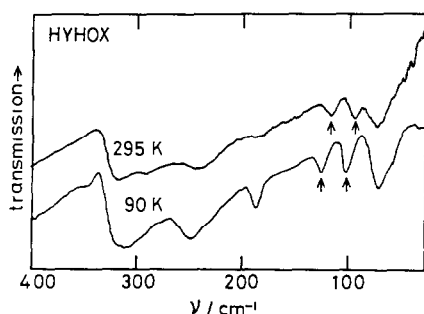


Fig. 6. Far-infrared spectra of hydrazinium hydrogen oxalate at 295 and 90 K. The arrows indicate the absorption peaks that shift to higher frequency at low temperature.

state. It comprises the proton-proton electrostatic interaction and elastic energy associated with the proton ordering. At present no attempt was made to interpret the energy in atomic terms.

In the far-infrared spectra of HYHOX (Fig. 6) we find two absorptions that shift markedly to a high frequency at low temperature. They are  $96\text{ cm}^{-1}$  (106) and  $118\text{ cm}^{-1}$  (129), the parenthesized frequencies being those at 90 K. Since the different frequencies give different vibrational heat capacities, we calculated the heat capacities of these oscillators at 217 K. The two modes gave  $0.016R$  for the difference of the heat capacities. This small effect does not change the Schottky level-calculation in any significant way. It is also probable that the effect of the changing frequencies has been taken into account in the fitting of the heat capacity and need not be considered separately.

## CONCLUSION

Rotational tunneling of  $-\text{CH}_3$  groups has been studied in many substances [18]. NMR and neutron scattering have established the occurrence of such a motion of the axial rotators in various environments. Translational tunneling is more difficult to detect and identify because it is coupled with other degrees of freedom of the crystal [19]. The analysis of the heat capacity presented here has ignored all the possible complications caused by interaction of the protons with the lattice vibrations. It is also known that the Ising model, on a linear chain, has a Schottky-like heat capacity [20]. But numerical comparison with the present data has not been made. Spectroscopic study of the motion of the acidic hydrogen is therefore desirable.

Apart from these finer details of the transition mechanism, the calorimetric data presented here have the following structural relevance. There has been controversy as to the accuracy and interpretation of the double peak electron distribution on the short hydrogen bonds [4,21]. It centers around whether or not the two peaks indicate two separate positions for a proton on the bond when a correction is made for the deformation of the electron cloud due to the bond formation. If a phase transition occurs, and its entropy change is of the order of  $R \ln 2$  as in the present case, it is most probable that the hydrogen bond is of the double minimum type even if the structural evidence is equivocal.

## ACKNOWLEDGEMENTS

The authors are indebted to Emeritus Professor Syûzô Seki for introducing them to experimental research in low temperature calorimetry in general and to the study of hydrogen-bonded systems in particular. His keen and

sustained interest in molecular interactions in the condensed phase is and has always been unfailing encouragement to them. One of the authors (T.M.) is grateful to J.O. Thomas for his illuminating discussion of the crystal structure of HYHOX.

## REFERENCES

- 1 N.A.K. Ahmed, R. Liminga and I. Olovsson, *Acta Chem. Scand.*, 22 (1968) 88.
- 2 A. Nilsson, R. Liminga and I. Olovsson, *Acta Chem. Scand.*, 22 (1968) 719.
- 3 J.O. Thomas, *Acta Crystallogr.*, Sect. B, 29 (1973) 1767.
- 4 J.O. Thomas and R. Liminga, *Acta Crystallogr.*, Sect. B, 34 (1978) 3684.
- 5 D. Hadzi and S. Bratos, in P. Schuster, G. Zundel and C. Sandorfy (Eds.), *The Hydrogen Bonds*, Vol. II, p. 568, North-Holland, Amsterdam, 1976.
- 6 G. Zundel, in P. Schuster, G. Zundel and C. Sandorfy (Eds.), *The Hydrogen Bonds*, Vol. II, North-Holland, Amsterdam, 1976, p. 683.
- 7 J. Lindgren, J. de Villepin and A. Novak, *Chem. Phys. Lett.*, 3 (1969) 84.
- 8 J. Tegenfeldt and I. Olovsson, *Acta Chem. Scand.*, 25 (1971) 101.
- 9 J.W. Harrell, Jr., R.A. Jensen and P.L. Gourley, *J. Magn. Reson.*, 33 (1979) 402.
- 10 J.W. Turrentine, *J. Am. Chem. Soc.*, 32 (1910) 577.
- 11 M. Tatsumi, T. Matsuo, H. Suga and S. Seki, *Bull. Chem. Soc. Jpn.*, 48 (1975) 3060.
- 12 Z. Mielke and H. Ratajczak, *J. Mol. Struct.*, 19 (1973) 751.
- 13 M.J. Schmelze, T. Miyazawa, S. Mizushima, T.J. Lane and J.W. Quagliano, *Spectrochim. Acta*, 9 (1957) 51.
- 14 H. Murata and K. Kawai, *J. Chem. Phys.*, 25 (1956) 589.
- 15 H. Murata, K. Kawai and J. Fujita, *J. Chem. Phys.*, 25 (1956) 796.
- 16 J. de Villepin and A. Novak, *Spectrochim. Acta*, Part A, 27 (1971) 1259.
- 17 J-O. Lundgren, R. Liminga and I. Olovsson, *Acta Chem. Scand.*, 25 (1971) 189.
- 18 W. Press, *Single Particle Rotations in Molecular Crystals*, Springer Verlag, Berlin, 1981.
- 19 M. Tokunaga and I. Tatsuzaki, *Phase Transitions*, 4 (1984) 97.
- 20 H.E. Stanley, *Introduction to Phase Transitions and Critical Phenomena*, Clarendon Press, Oxford, 1971.
- 21 M. Currie and J.C. Speakman, *J. Chem. Soc. A*, (1970) 1923.